Journal of Geoscience and Environment Protection, 2014, 2, 170-180
Published Online June 2014 in SciRes. http://www.scirp.org/journal/gep
http://dx.doi.org/10.4236/gep.2014.23022

SHRIMP U-Pb and U-Pb Laser Ablation Geochronological on Zircons from Monte Santo Alkaline Intrusive Suite, Westhern Araguaia Belt, Tocantins State, Brazil

Rúbia Ribeiro Viana, Gislaine Amorés Battilani

Department of Mineral Resource, Federal University of Mato Grosso, Cuiabá, Brazil
Email: rrviana@gmail.com, gislaine@ufmt.br

Received April 2014

Abstract

The Monte Santo Alkaline Intrusive Suite (MSAIS) is an association syenite foid, nepheline syenite and syenite, which are intruded in metapelites of the Rio do Coco meta-volcanic-sedimentary Sequence, presenting abundant pegmathoid veins cutting all of them. The ages obtained by Shrimp (1051 ± 22 Ma, 1048 ± 11 Ma) are very close those younger age obtained by U-Pb laser ablation (1056 ± 21), beeing interpreted as crystallization age. These dating reveal also that MSAIS rocks were affected by common succession of younger events below 550 Ma ago, responsible by the later rocky bodies of varying composition occurring in the region, including the alkaline pegmatites hosted in the nepheline syenite of the MSAIS.

Keywords

Alkaline Rocks, Shrimp Dating, Tocantins Structural Province, Neoproterozoic, Brazil

1. Introduction

Ancient alkaline rocks exposure is not common. There are few alkaline complexes such as the Canadian Shield (Superior Province), Greenland, Australia (Yilgarn Block) and South Africa is known. The oldest are found in Kirkland Lake region, Canada, dated of 2.7 Ga, represented by tracytos and leucite fonolite. As the generation the Neoproterozoic and Phanerozoic alkaline rocks occur in three main geodynamic settings: 1) continental rifts, 2) oceanic islands, and 3) subduction zones (peralkaline granites in back-arc zones). The Early Precambrian alkaline rocks formed at hotspots of the oceanic crust and are unknown in continental rifts (Sheth et al., 2002, Bonin, 1998; Blichert-Toft et al., 1996).

Ancient alkaline rocks are difficult to understand due to most Archean rocks are metamorphosed and some have undergone severe hydrothermal alteration, resulting in the destruction of the alteration-sensitive feldspathoids or alkaline mafic minerals that are diagnostic of alkaline magmatism. Alkaline lavas also may lose part of their alkalis and as a result appear more like ordinary tholeiites (Blichert-Toft et al., 1996).

How to cite this paper: Viana, R. R., & Battilani, G. A. (2014). SHRIMP U-Pb and U-Pb Laser Ablation Geochronological on Zircons from Monte Santo Alkaline Intrusive Suite, Westhern Araguaia Belt, Tocantins State, Brazil. *Journal of Geoscience and Environment Protection, 2,* 170-180. http://dx.doi.org/10.4236/gep.2014.23022

Precambrian alkaline rocks are sparsely distributed and outcrop relatively small areas scattered from north to south Brazil. These are not many studies about these rocks, being the main in alkalines rocks of Bahia (720 ± 9 to 732 ± 24 Ma Rosa et al., 2002, 2006; 2111 ± 13 Ma, Rios et al., 2007, 721 ± Ma Conceição et al., 2009), Rio Grande do Sul (615 ± 99 and 611 ± 3 Ma, Soliani Jr et al. 2000, Philipp et al. 2002), Pará (580 ± 10 and 724 ± 30 Ma, Jorge-João, 1980; Villas, 1982), Paraíba (*ca.* 600 to 580 Ma, Holland et al., 2009) and Tocantins (*ca.* 1500 Ma, Kitajima, 2002; Iwanuch, 1991).

In the Tocantins State, center-west of Brazil, are known three alkaline suites named of Estrela, Peixe and Monte Santo, therefore few detail studies of the petrogenetic and geochronological aspect were performed. This work is an attempt to characterize the age of the magmatism of the Monte Santo Alkaline Intrusive Suite (MSAIS), based in dating performed by Shrimp and laser ablation methods.

2. Geological Setting

The alkaline rocks studied in this work are positioned in the Tocantins Structural Province defined by Almeida (1977) and placed between San Francisco and Amazon Cratons. According to Pimentel et al. (2000) the Tocantins Structural Province represents a Brazilian orogen system characterized by belts of folds and thrusts called Brasilia, Paraguay and Araguaia belts, resulting from the convergence and collision of three continental blocks: the Amazon, San Francisco and Paranapanema cratons. In the study area neoproterozoic and basement rocks are partially covered by phanerozoic sediments of the Parnaíba Basin (Fuck et al., 2001). Paleoproterozoic basement rocks were partially reworked during the Brazilian orogeny (Pimentel et al., 2000).

The basement rocks in the area are represented by the core cratonic rocks with estimated ages between the Archean and Paleoproterozoic. It is composed by a granite-gneiss terrain affected by medium to high metamorphic degree associated with a metavolcanic-sedimentary sequence of the greenschist facies. According to Frasca & Araújo (2001) the cratonic unit represents the evolution of a portion of the rejuvenated crust re-mobilized and stabilized during the Paleoproterozoic. Structural features suggest a crustal unit independent represented by the Granite-Gneissic Rio dos Mangues Complex and by metavolcano-sedimentary Rio do Coco Sequence.

Frasca & Araújo (2001) reported that Monte Santo Alkaline Intrusive Suite is intruded in metapelites of the Rio do Coco meta-volcanic-sedimentary Sequence and in the Baixo Araguaia Group while Estrela Alkaline Suite outcrops accordingly with the rocks of the Rio dos Mangues Complex (**Figure 1**). Geochronological studies on zircons from syenitic gneisses by Pb-Pb method carried out by Souza & Moura (1996), indicated crystallization minimum ages of 1011 ± 86 Ma, interpreted as evidence of the beginning of the rifting process that generated the basin in which is deposited the Baixo Araguaia Group.

3. Analytical Techniques

In situ U-Pb analyses were performed on a SHRIMP-II instrument in the Center of Isotopic Research (CIR) at VSEGEI, Saint Petersburg, Russia. The results were obtained with a secondary electron multiplier in peak-jumping mode following the procedure described by Williams (1998). A primary beam of molecular oxygen was employed to bombard zircon in order to extract secondary ions. A 70 µm Kohler aperture allowed focusing of the primary beam so that the ellipse-shaped analytical spot had a size ca 25 µm × 20 µm, and the corresponding ion current was 5 nA. The sputtered secondary ions were accelerated at 10 kV. The 80 µm wide slit of the secondary ion source, in combination with a 100 µm multiplier slit, allowed mass-resolution M/ΔM ≥ 5000 (1% valley); thus, all the possible isobaric interferences were resolved. One minute rastering over a rectangular area of ca. 65 µm × 50 µm was employed before each analysis in order to remove the gold coating and any possible surface common Pb contamination. The following ion species were measured in sequence: 196(Zr_2O)-204Pb-background (ca 204 AMU)-206Pb-207Pb-208Pb-238U-248ThO-254UO with integration time ranging from 2 s to 14 s. Seven cycles for each analyzed spot were acquired. Apart from "unknown" zircons, each fourth measurement was carried out on the zircon Pb/U standard TEMORA 1, which has an accepted 206Pb/238U age of 416.75 ± 0.24 Ma (Black et al., 2003). The 91500 zircon standard, with U concentration of 81.2 ppm and a 206Pb/238U age of 1062 Ma (Wiedenbeck et al., 1995) was applied as the "U-concentration" standard. The results collected were then processed with the SQUID 1.02 (Ludwig, 2001) and Isoplot/Ex 3.00 (Ludwig, 2003) software, using the decay constants of Steiger and Jäger (1977). The common lead correction was done on the basis of measured 204Pb/206Pb and modern (*i.e.* 0 Ma) Pb isotope composition, according to the model of Stacey and Kramers (1975).

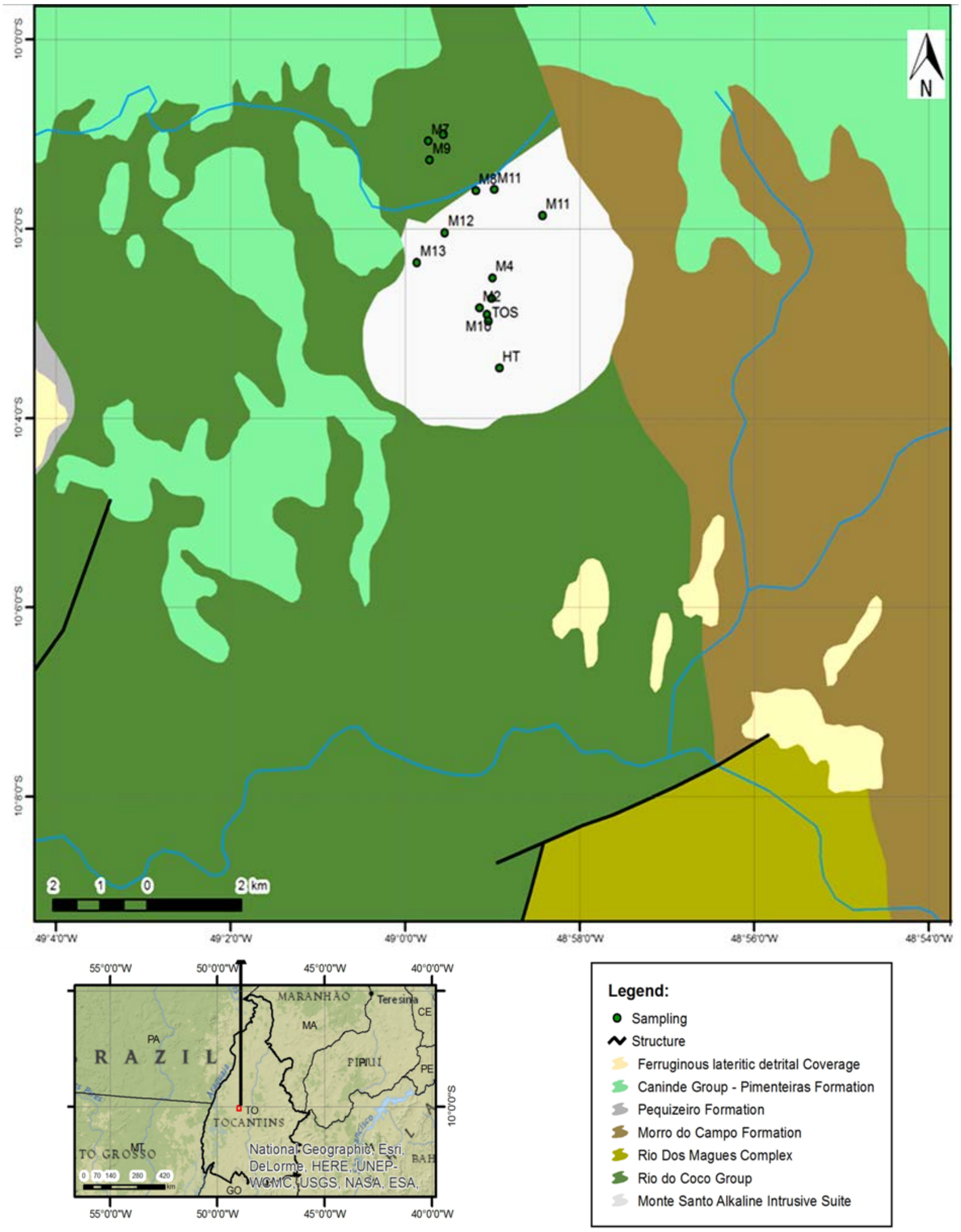

Figure 1. Geological sketch map of the Monte Santo Alkaline Intrusive Suite and adjacent rocks, Araguaia Belt, showing sample locations (modified from Gorayeb et al. (1996)).

The LA-MC-ICPMS analyses were performed in the Geological Survey of Finland where the chosen zircon grains were mounted in epoxy resin and sectioned approximately in half and polished. Back-scattered electron images (BSE) and cathodo luminescence (CL) images were prepared for the zircons to target the spot analysis sites. U-Pb dating analyses were performed using a Nu Plasma HR multicollector ICPMS in Espoo using a technique very similar to Rosa et al. (2009) except that a New Wave UP193 Nd: YAG laser microprobe was used. Samples were ablated in He gas (gas flow = 1.0 l/min) using a low volume teardrop-shaped (<2.5 cm^3) laser ablation cell (Horstwood et al., 2003). Raw data were corrected for background, laser induced elemental fractionation, mass discrimination and drift in ion counter gains and reduced to U–Pb isotope ratios by calibration to concordant reference zircons of known age, using protocols adapted from Andersen et al. (2004) and Jackson et al. (2004). Standard zircon GJ-01 (609 ± 1 Ma; Belousova et al., 2006) and an in-house standard A1772 (2711 ± 3 Ma/TIMS; 2712 ± 1 Ma/SIMS) were used for calibra-tion. For reference, either zircon A382 (1877 ± 2 Ma, Patchett and Kouvo, 1986) or A1933 (TIMS/1641 ± 2 Ma, SIMS/1640 ± 4 Ma) was run as an unknown to check the calibration. The calculations were done off-line, using an interactive spreadsheet pro-gram written in Micro-soft Excel/VBA by Tom Andersen (Rosa et al., 2009).

Plotting of the U-Pb isotopic data and age calculations were performed using the Isoplot/Ex 3 program (Ludwig, 2003). All the ages were calculated with 2σ errors and without decay constants errors. Data-point error ellipses in the figures are at the 2 σ level.

4. Description of the Selected Samples

A total of three samples (named of ABX, HPO_2 and HTOSN) were analyzed for the geochronology by Shrimp with two them also analyzed by laser ablation (ABX and HTOSN). All the samples present similar zircons with most of which preserved terminations. The backscattered electron (BSE) and cathodoluminescence (CL) imag-ing showed that larger grains have normally euhedral forms and can to present more deformed internal structure with a typical magmatic concentric or oscillatory zoning, while the smaller grains shows more altered blurry in-ternal structure, sometimes presenting massive interior structure to zoning marginal domain (**Figure 2**).

5. Results and Discussion

Five grains of zircon from the sample ABX were analyzed by shrimp (**Table 1** and **Figure 3**) and three grains using MC-LA-ICP-MS (**Table 2**). The Shrimp analyses showed that from five grains analyzed two of them (grains 2 and 3, **Table 1**) have two real ages of 1051 +/− 20 and 402 +/− 20 Ma (**Figure 3(a)**). All points of the

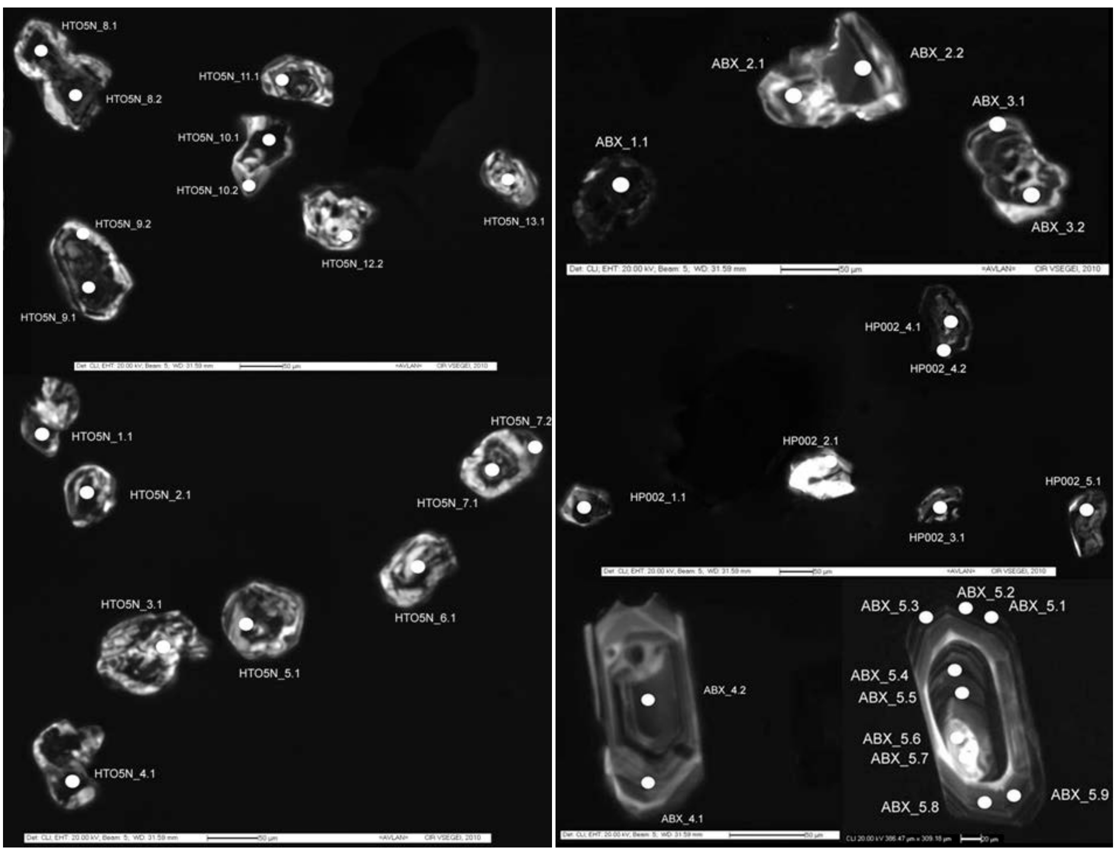

Figure 2. Cathodoluminescence images of selected zircon crystals separated from the studied rocks.

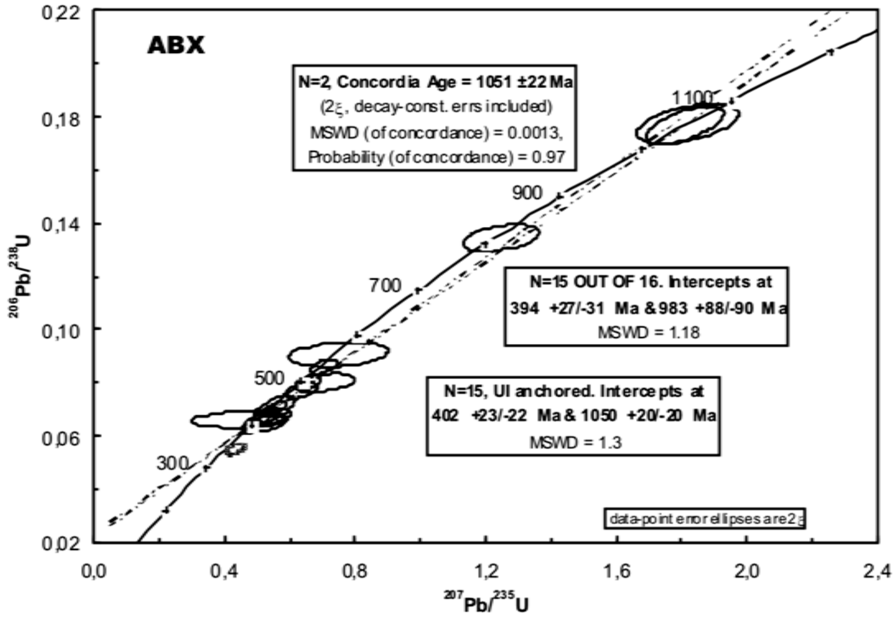

(a)

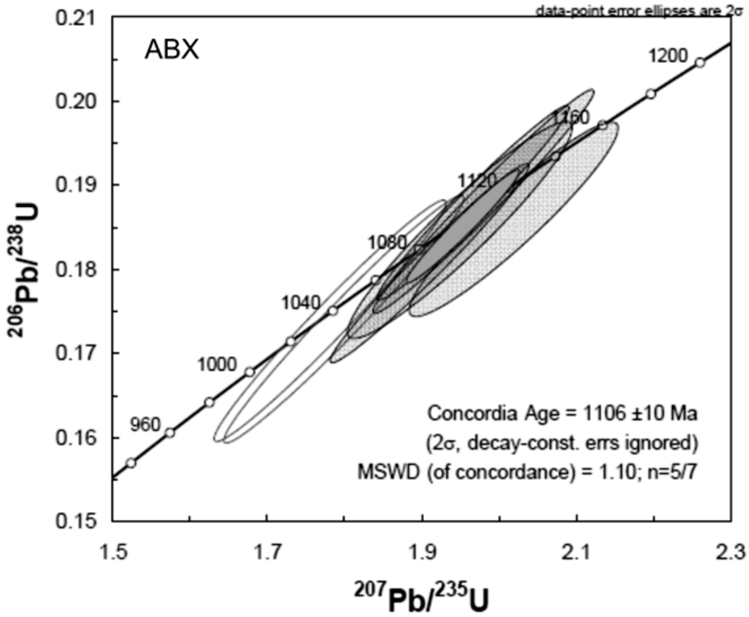

(b)

Figure 3. SHRIMP Zircon U-Pb Concordia plots and recalculated weighted mean 206Pb/238U ages (a) and MC-LA-ICPMS U-Pb (b) isotopic data for sample ABX from MSAIS rocks.

other grains analyzed showed ages close to those younger ages. The event of 520 Ma is not clearly registered. A big grain (grain 05) with nine spots analyzed, illustrate event of 400 - 420 Ma old (**Figure 3(a)**). By MC-LA-ICP-MS analyses, five analyses were done on the large grain and two on both the smaller grains, in which produced age of ~1100 Ma age for the two different types of zircon (**Table 2**, **Figure 3(b)**). In **Table 2** is also observed two discordant data points, it is not plotted in diagram.

From sample HTOS seventeen zircon grains were produced, in which thirteen were analyzed by shrimp (**Table 1**) and only four by MC-LA-ICP-MS (**Table 2**). Most of the zircon show many metamictic portions. The

Table 1. SHRIMP isotopic data for Zircon of the rocks from Monte Santo Alkaline Intrusive Suite.

Sample/ spot	% $^{206}Pb_c$	ppm U	ppm Th	ppm $^{206}Pb^*$	$\frac{^{232}Th}{^{238}U}$	(1) $\frac{^{206}Pb}{^{238}U}$ Age		(1) $\frac{^{207}Pb}{^{206}Pb}$ Age		%7 Dis-7cor-7dant	(1) $\frac{^{238}U}{^{206}Pb^*}$ ±%		(1) $\frac{^{207}Pb^*}{^{206}Pb^*}$ ±%		(1) $\frac{^{207}Pb^*}{^{235}U}$ ±%		(1) $\frac{^{206}Pb^*}{^{238}U}$ ±%		Errcorr
ABX_1.1	0.41	853	508	63.1	0.62	532	±7	581	±43	+9	11.6	1.3	0.0594	2.0	0.70	2.4	0.086	1.3	0.6
ABX_2.1	0.73	49	81	3.79	1.73	560	±11	601	±175	+7	11.0	2.1	0.0599	8.1	0.75	8.3	0.091	2.1	0.2
ABX_2.2	0.09	124	235	18.8	1.96	1050	±16	1050	±42	-0	5.7	1.6	0.0743	2.1	1.81	2.7	0.177	1.6	0.6
ABX_3.1	0.39	143	236	16.5	1.71	813	±12	848	±72	+4	7.4	1.6	0.0673	3.5	1.25	3.8	0.134	1.6	0.4
ABX_3.2	0.36	112	594	17.1	5.48	1053	±17	1051	±62	-0	5.6	1.7	0.0744	3.1	1.82	3.5	0.177	1.7	0.5
ABX_4.1	--	86	58	5.87	0.70	495	±8	746	±107	+35	12.5	1.8	0.0641	5.1	0.71	5.4	0.080	1.8	0.3
ABX_4.2	0.00	141	221	9.33	1.62	478	±7	603	±59	+21	13.0	1.6	0.0600	2.7	0.64	3.1	0.077	1.6	0.5
ABX_5.1	0.41	1475	340	69.5	0.24	344	±5	493	±52	+31	18.2	1.4	0.0570	2.4	0.43	2.7	0.055	1.4	0.5
ABX_5.2	--	702	246	42.5	0.36	439	±6	507	±43	+14	14.2	1.5	0.0574	1.9	0.56	2.4	0.070	1.5	0.6
ABX_5.3	--	678	231	46.4	0.35	495	±7	598	±38	+18	12.5	1.5	0.0599	1.8	0.66	2.3	0.080	1.5	0.6
ABX_5.4	0.34	403	115	24.2	0.29	436	±13	497	±78	+13	14.3	3.0	0.0571	3.5	0.55	4.7	0.070	3.0	0.7
ABX_5.5	0.17	553	134	31.9	0.25	419	±6	485	±56	+14	14.9	1.5	0.0568	2.5	0.53	2.9	0.067	1.5	0.5
ABX_5.6	1.28	118	49	6.69	0.43	411	±8	153	±312	-174	15.2	1.9	0.0491	13.3	0.45	13.4	0.066	1.9	0.1
ABX_5.7	0.00	100	38	5.52	0.39	403	±7	563	±95	+29	15.5	1.9	0.0589	4.4	0.52	4.7	0.065	1.9	0.4
ABX_5.8	0.26	352	165	20.3	0.49	420	±6	591	±71	+30	14.9	1.5	0.0597	3.3	0.55	3.6	0.067	1.5	0.4
ABX_5.9	0.00	470	192	26.4	0.42	408	±12	423	±55	+4	15.3	3.0	0.0553	2.5	0.50	3.9	0.065	3.0	0.8
HTOS_1.1	0.19	308	413	46.9	1.39	1052	±17	1050	±59	-0	5.6	1.7	0.0743	2.9	1.82	3.4	0.177	1.7	0.5
HTOS_2.1	0.17	384	461	57.8	1.24	1041	±16	1126	±30	+8	5.7	1.7	0.0772	1.5	1.87	2.3	0.175	1.7	0.7
HTOS_3.1	0.18	158	106	12.4	0.69	563	±9	593	±78	+5	11.0	1.6	0.0597	3.6	0.75	4.0	0.091	1.6	0.4
HTOS_4.1	--	395	187	58.8	0.49	1029	±16	1046	±28	+2	5.8	1.7	0.0742	1.4	1.77	2.2	0.173	1.7	0.8
HTOS_5.1	0.59	80	19	9.39	0.25	821	±14	921	±99	+11	7.4	1.8	0.0697	4.8	1.31	5.1	0.136	1.8	0.4
HTOS_6.1	1.06	67	71	10.1	1.10	1051	±19	1019	±115	-3	5.6	1.9	0.0732	5.7	1.79	6.0	0.177	1.9	0.3
HTOS_7.1	--	313	159	38.5	0.52	862	±14	1001	±76	+15	7.0	1.7	0.0725	3.7	1.43	4.1	0.143	1.7	0.4
HTOS_7.2	--	241	21	17	0.09	508	±7	582	±73	+13	12.2	1.5	0.0594	3.4	0.67	3.7	0.082	1.5	0.4
HTOS_8.1	0.16	480	619	73.6	1.33	1058	±14	1071	±26	+1	5.6	1.4	0.0751	1.3	1.85	1.9	0.178	1.4	0.7
HTOS_8.2	0.51	610	342	43.3	0.58	512	±7	550	±53	+7	12.1	1.4	0.0585	2.4	0.67	2.8	0.083	1.4	0.5
HTOS_9.1	0.08	338	123	50.3	0.38	1031	±14	1012	±28	-2	5.8	1.5	0.0729	1.4	1.74	2.0	0.173	1.5	0.7
HTOS_9.2	--	316	305	35.7	1.00	796	±11	932	±41	+15	7.6	1.5	0.0701	2.0	1.27	2.5	0.131	1.5	0.6
HTOS_10.1	--	498	463	67.3	0.96	943	±12	1044	±21	+10	6.4	1.4	0.0741	1.1	1.61	1.7	0.157	1.4	0.8
HTOS_10.2	0.86	154	33	12.2	0.22	568	±9	553	±147	-3	10.9	1.7	0.0586	6.7	0.74	6.9	0.092	1.7	0.2
HTOS11.1	--	340	298	51.8	0.91	1053	±14	1114	±33	+6	5.6	1.5	0.0767	1.6	1.88	2.2	0.177	1.5	0.7
HTOS_12.1	1.93	78	44	6.44	0.58	588	±12	354	±361	-69	10.5	2.2	0.0536	16.0	0.71	16.1	0.096	2.2	0.1
HTOS_13.1	1.34	195	255	15.8	1.35	581	±38	719	±121	+20	10.6	6.9	0.0633	5.7	0.82	8.9	0.094	6.9	0.8
HP002_2.1	2.66	39	81	2.83	2.15	523	±18	170	±783	-216	11.8	3.5	0.0495	33.5	0.58	33.7	0.085	3.5	0.1
HP002_6.1	29.37	3	19	0.132	6.24	301	±89	3293	±1213	+93	20.9	30.3	0.2677	77.3	1.76	83.0	0.048	30.3	0.4
HP002_6.2	0.40	525	122	30.4	0.24	421	±6	683	±55	+40	14.8	1.6	0.0623	2.6	0.58	3.0	0.068	1.6	0.5
HP002_4.1	3.48	398	696	24.1	1.81	440	±7	605	±201	+28	14.2	1.6	0.0600	9.3	0.58	9.4	0.071	1.6	0.2
HP002_4.2	0.96	305	81	22.7	0.27	535	±8	540	±109	+1	11.6	1.6	0.0583	5.0	0.69	5.2	0.086	1.6	0.3
HP002_1.1	--	347	88	26.6	0.26	550	±8	544	±55	-1	11.2	1.5	0.0584	2.5	0.72	2.9	0.089	1.5	0.5
HP002_5.1	0.25	218	136	30.9	0.64	985	±15	1020	±46	+4	6.1	1.6	0.0732	2.3	1.67	2.8	0.165	1.6	0.6
HP002_3.1	0.00	356	146	53	0.42	1030	±14	1098	±25	+7	5.8	1.5	0.0761	1.3	1.82	2.0	0.173	1.5	0.8

Errors are 1-sigma; Pb_c and Pb^* indicate the common and radiogenic portions, respectively. Error in Temora1 Standard calibration was 0.50%. (1) Common Pb corrected using measured 204Pb.

Table 2. MC-LA-ICP-MS isotopic data for Zircon of the rocks from monte santo alkaline intrusive suite.

Sample/spot	Feature spot	Age $\frac{^{207}Pb}{^{206}Pb}$		Age $\frac{^{207}Pb}{^{235}U}$		Age $\frac{^{206}Pb}{^{238}U}$		ratio $\frac{^{207}Pb}{^{206}Pb}$ (%)		ratio $\frac{^{207}Pb}{^{235}U}$ (%)		ratio $\frac{^{206}Pb}{^{238}U}$ (%)		(1)	(2) Discordant %	U ppm	Pb Ppm	$\frac{^{206}Pb}{^{204}Pb}$ measured	(3) f_{206}
ABX-1_1a	deformad zircon	1067	±14	1045	±23	1035	±33	0.0750	±0.0005	1.799	±0.064	0.1741	±0.0060	0.98	.	38	0	3.64E+03	0.07
ABX-1_1b	deformad zircon	1112	±10	1084	±18	1071	±27	0.0767	±0.0004	1.910	±0.053	0.1807	±0.0049	0.98	−1.2	103	0	1.24E+04	0.08
ABX-1_1c	deformad zircon	1104	±10	1108	±20	1111	±30	0.0763	±0.0004	1.979	±0.059	0.1881	±0.0055	0.98	.	126	0	1.42E+04	0.08
ABX-1_1d	deformad zircon	1166	±18	1122	±19	1099	±26	0.0788	±0.0007	2.019	±0.055	0.1859	±0.0048	0.94	−1.5	132	0	1.12E+04	0.08
ABX-1_1e	deformad zircon	1092	±10	1104	±17	1110	±26	0.0759	±0.0004	1.966	±0.051	0.1879	±0.0048	0.98	.	99	0	7.44E+03	0.08
ABX-1_2a	altered CL-spotty	1110	±19	1098	±20	1092	±29	0.0766	±0.0008	1.949	±0.059	0.1846	±0.0053	0.94	.	14	0	1.73E+03	0.08
ABX-1_2b	*altered CL-spotty*	*1050*	*±14*	*1039*	*±22*	*1034*	*±32*	*0.0743*	*±0.0005*	*1.782*	*±0.061*	*0.1739*	*±0.0059*	*0.98*	.	*41*	*0*	*3.65E+03*	*0.07*
ABX-1_3a	*altered CL-dark*	*735*	*±14*	*482*	*±14*	*430*	*±15*	*0.0638*	*±0.0005*	*0.607*	*±0.022*	*0.0690*	*±0.0024*	*0.98*	*−39.9*	*38*	*0*	*4.53E+03*	*0.06*
ABX-1_3b	altered CL-dark	1002	±22	543	±16	440	±16	0.0726	±0.0008	0.706	±0.027	0.0706	±0.0026	0.96	−55.2	11	0	2.42E+04	0.07
HTOS-_1[a]	*altered CL-spotty*	*947*	*±19*	*747*	*±26*	*682*	*±32*	*0.0707*	*±0.0007*	*1.087*	*±0.054*	*0.1116*	*±0.0055*	*0.98*	*−25,2*	*36*	*0*	*2.52E+03*	*0.07*
HTOS_1b	altered CL-spotty	1045	±14	1049	±28	1051	±40	0.0741	±0.0006	1.810	±0.076	0.1771	±0.0073	0.98		22	0	1.67E+03	0.07
HTOS_1d	altered CL-spotty	1049	±15	1018	±29	1004	±41	0.0743	±0.0006	1.726	±0.078	0.1686	±0.0075	0.99	−0.4	66	0	4.63E+03	0.07
HTOS_2[a]	altered CL-spotty	1056	±11	984	±27	952	±37	0.0745	±0.0004	1.636	±0.070	0.1592	±0.0067	0.99	−7.9	114	0	2.44E+05	0.07
HTOS_2b	altered CL-spotty	1080	±11	1031	±26	1009	±38	0.0754	±0.0004	1.761	±0.072	0.1694	±0.0068	0.99	−4.4	103	0	4,70E+04	0.08
HTOS_3[a]	*CL-dark/BSE-spotty*	*1258*	*±10*	*780*	*±27*	*623*	*±30*	*0.0825*	*±0.0004*	*1.155*	*±0.058*	*0.1015*	*±0.0051*	*1.00*	*−51.8*	*228*	*1*	*2.11E+03*	*0.08*
HTOS_3b	*CL-dark/BSE-spotty*	*1215*	*±13*	*783*	*±28*	*641*	*±31*	*0.0807*	*±0.0005*	*1.163*	*±0.059*	*0.1045*	*±0.0053*	*0.99*	*−48.0*	*324*	*1*	*1.88E+03*	*0.08*
HTOS_3c	*CL-dark/BSE-spotty*	*1141*	*±10*	*727*	*±26*	*600*	*±29*	*0.0778*	*±0.0004*	*1.046*	*±0.053*	*0.0975*	*±0.0049*	*1.00*	*−48.4*	*315*	*1*	*1.07E+03*	*0.08*
HTOS_4[a]	*CL-pale/BSE-dark blurry*	*1191*	*±47*	*1068*	*±34*	*1909*	*±43*	*0.0798*	*±0.0019*	*1.864*	*±0.097*	*0.1695*	*±0.0078*	*0.89*	*−6.0*	*3*	*0*	*3.00E+02*	*0.08*
HTOS_4b	*CL-pale/BSE-dark blurry*	*833*	*±59*	*998*	*±40*	*1075*	*±55*	*0.0669*	*±0.0020*	*1.673*	*±0.105*	*0.1816*	*±0.0100*	*0.88*	8.4	*2*	*0*	*2.24E+02*	*0.07*

All errors are in 1sigma level. Data in italic and strikethrough are rejected mainly because of high common lead contents. Data in italic are ignored in diagrams due to high discordancy.1)Error correlation in conventional Concordia space. 2) Age discordance at closest approach of error ellipse to Concordia. 3) Percentage of common $_{206}$Pb in measured $_{206}$Pb, calculated from the $_{204}$Pb signal assuming a present-day Stacey & Kramers (1975) model terrestrial Pb-isotope composition.

shrimp analyzed have a very good example of two ages in the single crystal, which is shown in grains 7, 8, 9 and 10 (**Table 2**). Both ages are concordant and are of 1048 ± 11 and 511 ± 10 Ma (**Figure 4(a)**). A total of ten MC-LA-ICP-MS analysis were realized and revealed all the spots analyzed of the zircon 03 and one from zircon 01 showed highly discordant age (**Table 2**). The remaining analyses produced equivalent U-Pb age of approximating1060 Ma (**Figure 4(b)**).

The sample HPOO2 had their zircon analyzed only by Shrimp, in the total of six grains. The grain 4 is the unique that revel two real ages of 1030 ± 14 e another of 535 ± 8, Ma (**Table 2**, **Figure 5**). The last event is stronger and it was influenced for other younger (ca 420 Ma).

The ages obtained by MC-LA-ICP-MS and Shrimp method show ages very close. The studied samples were characterized by common succession of events, with the Shrimp crystallization age varying of 1051 ± 22 Ma and 1048 ± 11 Ma and MC-LA-ICP-MS ages varying of 1106 ± 10 Ma and 1056 ± 21 Ma, with subsequent re-crystallization during much younger process below 500 Ma ago.

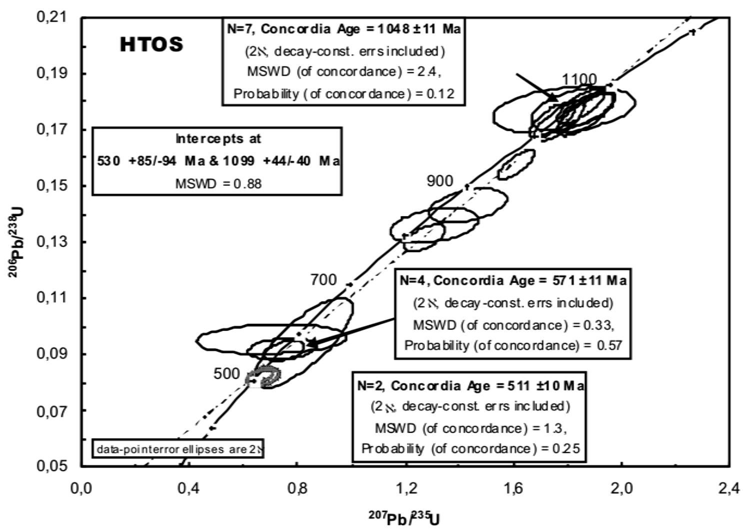

(a)

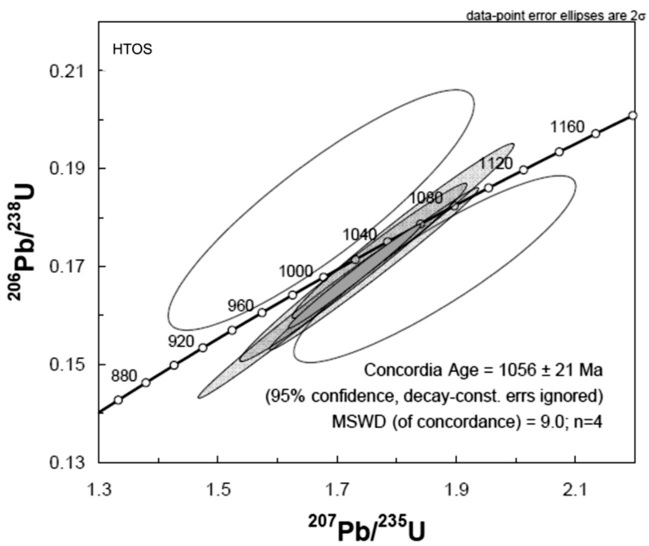

(b)

Figure 4. SHRIMP Zircon U–Pb Concordia plots and recalculated weighted mean 206Pb/238U ages (a) MC-LA-ICPMS U-Pb isotopic data for sample HTOS from MSAIS rocks.

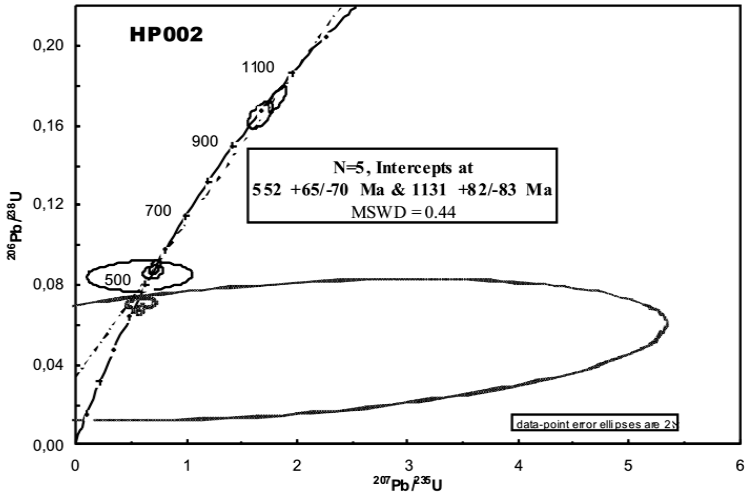

Figure 5. SHRIMP Zircon U-Pb Concordia plots and recalculated weighted mean 206Pb/238U ages.

We interpret the concordant older ages as recording the time of crystallization of zircon in the Alkaline Monte Santo Complex. Although some grains seems have been affected by cracks, no evidence from the analytical data was found to be anomalous.

The crystals subsequently affected by one or more episodes of lead loss, suggesting that the nepheline syenitic rocks have been involved in a thermo-tectonic episode, namely Brazilian Orogeny, in the end of the Neoproterozoic. These events are represented by concordant ages of 511 ± 10, 535 ± 8 and 402 ± 20 Ma and may have been responsible for the granitegenesis described by Alvarenga et al. (2000) in domain of Estrondo Group and also for the reactivation of numerous fractures occurred to south, as well as by the intense hydrothermal activity and metasomatic alterations in which modify the primary mineralogy of the rocks of the Monte Santo Alkaline Intrusive Suite. These episodes were also responsible by generation of the later bodies and including the alkaline pegmatites present in the area.

Acknowledgements

This work was partially supported by the Foundation for Research Support of the State of Mato Grosso (FAPEMAT) and National Scientific and Technological Development Council (CNPQ).

References

Almeida, F. F. M., Hasui, Y., Brito Neves, B. B., & Fuck R. A. (1977). Províncias Estruturais Brasileiras. *VIII Simpósio de Geologia do Nordeste, Campina Grande*, Atas. Pernanbuco, SBG—Núcleo Nordeste, 1, 363-392.

Alvarenga, C. J. S., Moura, C. A. V., Gorayeb, P. S. S., & Abreu, F. A. M. (2000). Paraguai and Araguaia belts. In U. G. Cordani, E. J. Milani, A. Thomaz Filho, & D. A.Campos (Eds.), Tectonic Evolution of South America, 183-193.

Andersen, T., Griffin, W. L., Jackson, S. E., Knudsen, T.-L., & Pearson, N. J. (2004). Mid-Proterozoic Magmatic Arc Evolution at the Southwest Margin of the Baltic Shield. *Lithos, 73,* 289-318. http://dx.doi.org/10.1016/j.lithos.2003.12.011

Belousova, E. A., Griffin, W. L., & O'Reilly, S. Y. (2006). Zircon Crystal Morphology, Trace Element Signatures and HF Isotope Composition as a Tool for Petrogenetic Modeling: Examples from Eastern Australian Granitoids. *Journal of Petrology, 47,* 329-353. http://dx.doi.org/10.1093/petrology/egi077

Black, L. P., Kamo, S. L., Allen, C. M., Aleinikoff, J. N., Davis, D. W., Korsch, R. J., & Foudoulis, C. (2003). TEMORA 1: a New Zircon Standard for Phanerozoic U-Pb Geochronology. *Chemical Geology, 200,* 155-170. http://dx.doi.org/10.1016/S0009-2541(03)00165-7

Blichert-Toft, J., Arndt N. T., & Ludden, J. N. (1996). Precambrian Alkaline Magmatism. *Lithos, 37,* 97-111. http://dx.doi.org/10.1016/0024-4937(95)00031-3

Bonin, B., Azzouni-Sekkal, A., Bussy, F., & Ferrag, S. (1998). Alkali-Calcic and Alkaline Post-Orogenic (PO) Granite Magmatism: Petrologic Constraints and Geodynamic Settings. *Lithos, 45,* 45-70.

http://dx.doi.org/10.1016/S0024-4937(98)00025-5

Conceição, H., Rosa, M. L. S., Moura, C. A. V., Macambira, M. J. B., Galarza, M. A., Rios, D. C., Marinho, M. M., Menezes, R. C. L., & Cunha, M. P. (2009). Petrology of the Neoproterozoic Itarantim Nepheline Syenite Batholith, São Francisco Craton, Bahia, Brazil. *Can Mineral, 47,* 1527-1550. http://dx.doi.org/10.3749/canmin.47.6.1527

Frasca, A. A. S., & Araújo, V. A. (2001). *Projeto Hidrogeologia no Tocantins—Folha Palmas—SD 22-Z-B*. Goiânia: CPRM/Serviço Geológico do Brasil, 52 p.

Fuck, R. A., Dantas, E. L., Pimentel, M. M., Junges, S. L., & Moraes, R. (2001). Nd isotopes, U–Pb single grain and SHRIMP zircon ages from basement rocks of the Tocantins Province. *Proceedings of the III South American Symposium on Isotope Geology*, Santiago, Extended Abstract, 141-144 (CD ROM).

Gorayeb P. S. S. (1996). *Petrologia e evolução crustal das rochas de alto grau de Porto Nacional—TO*. Tese de Doutorado. Belém: Instituto de Geociências, Universidade Federal do Pará, 258 p.

Holland, M. H. B. M., Mejía, C. P., Archanjo, C. J., & Armstrong, R. (2009). Geologia e Caracterização Química do Magmatismo Peralcalino Ultrapotássico do Enxame de Diques Manaíra-Princesa Isabel, Província Borborema. *Geol. USP, Sér. cient., São Paulo, 9,* 13-46.

Horstwood, M. S. A., Foster, G. L., Parrish, R. R., Noble, S. R., & Nowell, G. M. (2003). Common-Pb Corrected *in Situ* U-Pb Accessory Mineral Geochronology by LA-MC-ICP-MS. *Journal of Analytical Atomic Spectrometry, 18,* 837–846. http://dx.doi.org/10.1039/b304365g

Iwanuch, W. (1991). *Geologia dos complexos alcalinos proterozóicos do centro do estado de Tocantins.* Tese de Doutorado; São Paulo: Instituto de Geociências, Universidade de São Paulo, 202 p.

Jackson, S. E., Pearson, N. J., Griffin, W. L., & Belousova, E. A. (2004). The Application of Laser Ablation-Inductively Coupled Plasma-Mass Spectrometry to *In-Situ* U-Pb Zircon Geochronology. *Chemical Geology, 211,* 47-69. http://dx.doi.org/10.1016/j.chemgeo.2004.06.017

Jorge-João, X. S. (1989) *O litchfieldito Boca Nova no nordeste do Estado do Pará: Aspectos petroquímicos e implicação econômica*. Belém: CPRM.

Kitajima, L. F. W. (2002). *Mineralogia e petrologia do Complexo Alcalino de Peixe—Tocantins*. Tese Instituto de Geociências, Universidade de Brasília.

Ludwig, K. R. (2001). *SQUID 1.02, A User Manual, A Geochronological Toolkit for Microsoft Excel.* Berkeley: Berkeley Geochronology Center Special Publication.

Ludwig, K. R. (2003). *User's Manual for Isoplot/Ex, Version 3.00, A Geochronological Toolkit for Microsoft Excel.* Berkeley: Berkeley Geochronology Center Special Publication.

Patchett, J., & Kouvo, O. (1986). Origin of continental crust of 1.9-1.7 Ga age: Nd iso-topes and U-Pb zircon ages in the Svecokarelian terrain of south Finland. *Contributions to Mineralogy and Petrology, 92,* 1-12. http://dx.doi.org/10.1007/BF00373959

Philipp, R. P., Machado, R., Nardi, L. V. S., & Lafon, J. M. (2002). O magmatismo granítico neoproterozóico do BatólitoPelotas no sul do Brasil: Novos dados e revisão da geocronologia regional. *Rev Bras Geoc, 32,* 277-290.

Pimentel, M. M., Fuck, R. A., Jost, H., Ferreira Filho, C. F., & Araújo, S. M. (2000). The basement of the Brasília Fold Belt and the Goiás Magmatic Arc. In U. G. Cordani, E. J. Milani, A. Thomaz Filho, & D. A. Campos (Eds.), *Tectonic Evolution of South America* (pp. 190-229). Rio de Janeiro: 31st IGC,

Rios, D. C., Conceição, H., Davis, D. W., Plá Cid, J., Rosa, M. L. S., Macambira, M. J. B., Mcreath, I., Marinho, M. M., & Davis, W. J. (2007). Paleoproterozoic potassic-ultrapotassic magmatism: morro do afonso syenite pluton, bahia, brazil. *Precambrian Research, 154,* 1-30. http://dx.doi.org/10.1016/j.precamres.2006.11.015

Rosa, D. R. N., Finch, A. A., Andersen, T., & Inverno, C. M. C. (2009). U-Pb Geochronology and Hf Isotope Ratios of Magmatic Zircons from the Iberian Pyrite Belt. *Mineralogy and Petrology, 95,* 47-69. http://dx.doi.org/10.1007/s00710-008-0022-5

Rosa, M. L. S., Conceicão, H., Macambira, M. J. B., Galarza, M. A., Cunha, M. P., Menezes, R. C. L., Marinho, M. M., Cruz Filho, B. E., & Rios, D. C. (2007). Neoproterozoic Anorogenic Magmatism in the Southern Bahia Alkaline Province of NE Brazil: U-Pb and Pb-Pb Ages of the Blue Sodalite Syenites. *Lithos,* 88-97. http://dx.doi.org/10.1016/j.lithos.2006.12.011

Rosa, M. L. S., Conceição, H., Marinho, M. M., Macambira, M. J. B., & Marques, L. S. (2002). Geochronology of the South Bahia Alkaline Province (NE Brazil). *Geochimica et Cosmochimica Acta, 66,* A648.

Sheth, H. C., Torres-Alvarado, I. S., & Verma, S. P. (2002). What Is the Calc-Alkaline Rock Series? *International Geology Review, 44,* 686-701. http://dx.doi.org/10.2747/0020-6814.44.8.686

Soliani, J. R. E., Koester, E., & Fernandes, L. A. D. (2000). A geologia isotópica do Escudo Sul-rio-grandense—Parte I: métodos isotópicos e valor interpretativo. In M. Holz, & L. F. Deros (Eds.), *Geologia do Rio Grande do Sul* (pp. 175-230).

Volume Especial do CIGO/UFRGS. Porto Alegre.

Villas, R. N. N. (1982). Geocronologia das intrusões ígnea na bacia do rio Guamá, nordeste do Estado do Pará. In: Simpósio de Geologia da Amazônia, 2, Belém, *Anais.* Belém, SBG, 1, 233-247.